ARCHIVE OF MECHANICAL ENGINEERING

DOI: 10.24425/ame.2025.153735 Early Access; pp. 1–22

Shekhar NISHAD [1], Krishna Prasad MADASU [1]

Thermophoresis of an aerosol cylinder in Brinkman medium within a cylindrical cavity

Received 27 August 2024, **Revised** 31 January 2025, **Accepted** 3 February 2025, **Published online** 11 February 2025

Keywords: thermophoresis, aerosol cylinder, cylindrical cavity, continuum regime, Brinkman medium

This work presents the thermophoretic migration of a solid cylinder, whose direction is normal to its axis and situated in a concentric cylindrical cavity. The space between the particle and the cavity is filled with isotropic porous medium. The Kundsen number is considered to be small, so that the fluid flow through the porous medium is in continuum regime. The continuity of heat flux, temperature jump, viscous slip, thermal creep and thermal stress slip conditions are employed to solve the thermal transport and fluid flow equations. We have obtained analytical expressions for thermophoretic velocity, thermophoretic mobilities and drag force. The effects of the permeability, frictional slip parameter, particle-to-cavity radii ratio, and thermal conductivity ratio of particle to medium on thermoosmotic velocity, thermophoretic mobility and net normalized velocity are presented in graphical form. We have found that the thermoosmotic and thermophoretic mobility have maximum for the high permeability, and for the low radii ratio of particle to cavity. Reduction cases for the unbounded medium are also obtained. The present study has significant applications in industrial and engineering fields, such as manufacturing of precipitators, sampling of soot particles, air cleaning, etc.

Nomenclature

a Radius of inner cylinder, m
b Radius of outer cylinder, m
k_p Thermal conductivity of the particle, $\mathrm{Wm^{-1}K^{-1}}$
k_w Thermal conductivity of the cavity, $\mathrm{Wm^{-1}K^{-1}}$
k_p^* Thermal conductivity ratio of the particle to the medium

✉ Krishna Prasad MADASU, emails: madaspra.maths@nitrr.ac.in, kpm973@gmail.com
Shekhar NISHAD, email: snishad.phd2022.maths@nitrr.ac.in
[1]Department of Mathematics, National Institute of Technology Raipur, Chhattisgarh, India

k_w^* Thermal conductivity ratio of the cavity to the medium
T_p The temperature distribution for the cylindrical particle, K
T The temperature distribution for the porous medium, K
T_w The temperature distribution for the cavity surroundings, K
E_∞ The prescribed temperature gradient in the absence of the particle, Km^{-1}
C_t The temperature jump coefficient of the particle surface
C_t' The temperature jump coefficient of the cavity wall
C_m The frictional slip coefficient of the particle surface
C_m' The frictional slip coefficient of the cavity wall
C_s, C_s' The thermal creep coefficients of the particle surface and cavity wall
C_h, C_h' The thermal stress slip coefficients of the particle surface and cavity wall
k_1 The permeability, m^2
u_ρ, u_θ Components of fluid velocity in cylindrical coordinates ms^{-1}
$\vec{u}$ Fluid velocity ms^{-1}
U Translational velocity of the particle, ms^{-1}
T_0 Absolute temperature at the position of particle center in the absence of the particle, K
T_∞ Prescribed temperature distribution in the absence of the particle, K
F_T Drag force exerted on the cylindrical particle, N
l Mean free path of the gas molecules, m
p Dynamic pressure distribution, Nm^{-2}
$\vec{e}_\rho$, $\vec{e}_\theta$ Unit vectors in ρ and θ directions
$\vec{e}_x$ Unit vector in $x-$ direction
U_T Thermophoretic velocity, ms^{-1}
U_{os} Thermoosmotic velocity, ms^{-1}
M_T Thermophoretic mobility constant
$K_n(*)$ The modified Bessel's function of order n

Greek letters

α The permeability parameter
μ Viscosity of the fluid, $\mathrm{kgm}^{-1}\mathrm{s}^{-1}$
λ Radii ratio of particle to cavity
ρ_A Density of the fluid, kgm^{-3}
ρ Radial cylindrical coordinate, m
θ Angular cylindrical coordinate
ψ Stream function, $\mathrm{m}^3\mathrm{s}^{-1}$
∇^2 Laplacian operator
$t_{\rho\rho}$ Normal stress in porous medium, Nm^{-2}
$t_{\rho\theta}$ Shear stress in porous medium, Nm^{-2}

1. Introduction

It is generally known that when a microparticle is suspended in a gaseous medium under a uniform temperature gradient, the particle experiences a force that causes it to move towards the regions of decreasing temperature. This phenomenon

is known as thermophoresis. The phenomenon was first described by Tyndall, who observed a dust-free zone surrounding a hot body [1]. Later, Maxwell provided a physical explanation of thermophoresis [2]. In the hotter region, gas molecules possess more momentum than those in the colder region, leading to the movement of particles in the opposite direction to the temperature gradient.

In industrial and technical sectors, thermophoresis is significant for studying the mechanisms involved in capturing soot particles on cold surfaces. This has applications in air purification, microelectronics production, nuclear reactor safety, chemical vapor deposition, and the design of microscale thermophoretic turbines, sampling of aerosol particles [3–7]. Theoretical and experimental investigations [8] have been conducted to understand the behavior of particle under thermophoresis. The experimental data have shown that the Knudsen number plays a crucial role in thermophoresis, which is defined as the ratio of the mean free path of the gas molecules to the radius of the particle and denoted by $Kn = l/a$. Using the perturbation technique and considering low Péclet, Reynolds and Knudsen numbers, Brock [9] have found the expression for thermophoretic velocity of an aerosol sphere in an unbounded viscous fluid under uniform temperature gradient. He observed that the thermophoretic velocity of the particle is a function of the relevant parameters, including the thermal properties, jump, and slip characteristics of both the particle and the medium.

In recent years, many researchers have discussed the thermophoresis problems of various shaped particles in viscous fluids. Leong [10] studied the thermophoresis of spheroidal particle by appealing to the prolate and oblate spheroidal coordinate systems. Chang and Keh [11] analyzed the thermophoretic behavior of a deformed aerosol sphere. Maghsoudi et al. [12] discussed the flow past a heating circular cylinder in an unbounded gaseous medium by applying temperature jump and slip conditions. Keh and Tu [13] studied the thermophoretic migration of an aerosol cylinder in an unbounded gaseous medium oriented perpendicular to the uniform thermal gradient. Sone [14] and Lockerby [15] described the thermal stress slip that represents the second-order temperature gradient at the solid surface. Chang and Keh [16] analyzed the thermophoresis problem of an aerosol sphere by considering thermal stress slip condition. They obtained the drag force exerted on an aerosol sphere in good agreement with the experimental data and compared the results of Brock [9] and Mackowski [17] with zero thermal stress slip condition. Chang and Keh [18] studied the thermophoresis of cylindrical particle in unbounded viscous fluid by assuming thermal stress slip and determined the expression for the thermophoretic velocity in uniform temperature gradient given as

$$U = \frac{\mu E_\infty}{\rho T_0} \frac{(1 + k\, C_t\, l/a)\,(C_s + (1-k)\, C_h\, C_m\, l/a)}{(1 + 2\, C_m\, l/a)\,(1 + k + k\, C_t\, l/a)}, \tag{1}$$

where μ, ρ are viscosity and density of the medium, respectively; k is the thermal conductivity ratio of particle to the medium; C_t, C_m, C_s, C_h denote the temperature jump, viscous slip, thermal creep and thermal stress slip coefficients at the particle

surface, respectively. E_∞ is a uniform temperature gradient, and T_0 is the prescribed temperature at the axis of the cylinder (or the mean gas temperature in the vicinity of the particle). Using the singular perturbation method, Tseng et al. [19] found the thermophoretic velocity of the cylindrical particle suspended in a gaseous medium with the consideration of non-zero Péclet number. When the force is driven by both temperature and concentration gradients, the force is referred to as the general thermophoretic force. It arises from the collisions between gas molecules and particles that are suspended in the gas. Dung [20] derived the expression for the general thermophoretic force of a spherical particle suspended in a gaseous medium. Bashir et al. [21] examined the thermophoresis phenomenon in the context of the electrically conducting flow of viscous fluids around a revolving and vertically moving permeable disk and discussed the thermal characteristics of medium.

It is seen that the fluid flow in the bounded medium is extremely important, such as fluid flow through channels and micro annular tubes have many applications in chemical separations, biomedical, medical, and computer chips, etc. Bhatti et al. [22] discussed the third-grade nanofluid between vertical channels under the effect of electric and magnetic fields. They have applied the shooting method to find the numerical outcomes for the temperature and velocity fields. Sarkar and Madasu [23] studied the parallel and perpendicular flow of couple stress fluid past a circular cylinder using the cell model technique. Marin [24] assessed the unique solution of mixed problem for thermoelastic theory in which the heat conduction is estimated by the Moore-Gibson Thompson equation. Many researchers have discussed the thermophoretic mobility of aerosol particles in the presence of boundaries due to its wide range of applications. Keh and Chang [25] analyzed the effects of boundary on Stokes flow and thermophoretic migration of a spherical particle within a spherical cavity. Keh and Ho [26] explored the effects of concentration on the thermophoretic motion of spherical particle in the bounded medium using the cell model technique. Recently, Li and Keh [27] discussed the thermophoretic migration of a spherical particle within a cavity filled with viscous fluid. The motion of a spherical particle situated eccentrically in the spherical cavity with the presence of Newtonian fluid has been discussed in refs. [28, 29]. Using the optimal homotopy analysis method, Shah et al. [30] explored the second-grade fluid flow through a vertical plate under the effects of thermophoresis and magnetic field. Sarfraz et al. [31] examined the stagnation flow of nanofluid that arises due to twisting motion of a cylinder in the presence of magnetic field, thermophoresis and Brownian motion.

The fluid flow through a homogenous porous medium represents many real-world applications such as sedimentation, soil contamination, oil recovery and filtration processes in industries, etc. [32–34]. Faltas et al. [35] discussed the thermophoretic migration of a spherical particle situated between two permeable channels. Faltas and Ragab [36] studied the thermophoretic migration of a cylindrical particle in an unbounded Brinkman medium and obtained the analytical expressions of thermophoretic velocity and thermophoretic force. Ayman et al.

[37] investigated the effect of concentration on the motion of spherical particle in an unbounded Brinkman medium under the temperature gradient. Faltas et al. [38] considered the non-zero Péclet number for studying the thermophoretic migration of spherical particle immersed in a Brinkman medium. The thermophoresis problems related to the motion of spherical particle in a spherical cavity filled with porous media for the concentric and eccentric cases have been studied in the refs. [35, 39]. This type of particle movement in the cavity can be used as a model to capture soot particles employing thermophoresis in porous filters made up of pores. These results encourage us to conduct the current study and explore the thermophoretic behavior of cylindrical particle in a cylindrical cavity filled with Brinkman medium. To the best of author's knowledge, the current study has not been conducted before.

The primary goal of this paper is to analyze the thermophoretic motion of a cylindrical particle positioned concentrically within a cylindrical cavity. Additionally, it aims to investigate the effects of permeability, thermal properties, and slip parameters of the particle and surrounding medium on the thermophoretic migration of the particle in a Brinkman medium. This study extends the work by Faltas and Ragab [36] to the case of the bounded medium. The exploration of this topic will assist industrial professionals in effectively removing dust particles from filters and precipitators under temperature gradient. In this work, we examine the behavior of a cylindrical particle within a cylindrical cavity that contains pores. The results indicate that the movement of the particle is influenced by the medium's physical, thermal, and permeability properties.

2. Thermophoresis

Consider the thermophoresis of a large circular cylindrical particle of radius a and of thermal conductivity k_p placed in a concentric cylindrical cavity of radius b and of thermal conductivity of wall k_w, as illustrated in Fig. 1. The gap is filled with homogenous porous medium where overall thermal conductivity is k_A.

Consider a uniform temperature gradient $\nabla T_\infty (= -E_\infty \vec{e}_x)$ is maintained at a distance far from the particle. Where $\vec{e}_x$ is the unit vector in the $x-$direction and $E_\infty > 0$. Let (ρ, θ, z) and (x, y, z) be a cylindrical and Cartesian coordinate system originating O from the center of the particle with $(\vec{e}_\rho, \vec{e}_\theta, \vec{e}_z)$, and $(\vec{i}, \vec{j}, \vec{k})$ are the corresponding unit vectors, respectively. The axis of cylinder is along $z-$ direction, and the cylinder is moving in $x-$ direction with uniform velocity U, which needs to be determined. For the current work, the following assumptions are considered:

- The flow is steady, incompressible and axisymmetric.
- The porous medium is homogenous and isotropic.
- The Kundsen number is small.
- The Reynolds and Péclet numbers are negligible.
- All the physical properties of the particle and fluid are assumed to be constants.

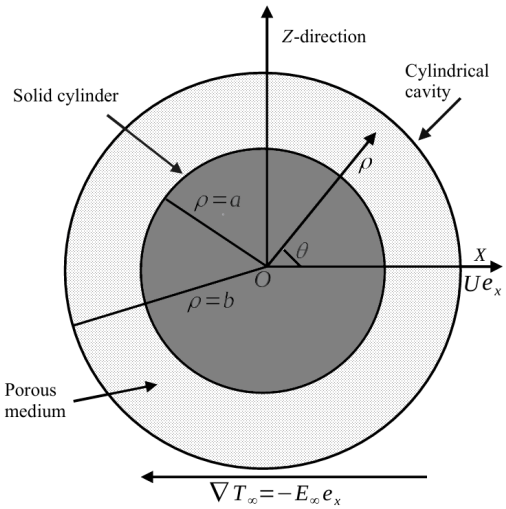

Fig. 1. Physical representation of the problem

- The thermal slip over a particle in the continuum regime (the Knudsen number $l/a << 1$ where l is the mean free path of the gas molecules and a is radius of the particle).

Based on above assumptions, the temperature and flow fields of the system are governed by Laplace's and Brinkman's equations, respectively.

To solve for the thermophoretic motion of the cylindrical particle in a cylindrical cavity, one first needs to solve for the system temperature field.

2.1. Thermal transport distributions

Energy equation describing the fluid flow through porous medium are mentioned in refs. [36, 40]. The governing equations for temperature distributions T_p for inside the particle, T for the porous medium, and T_w for outside the cavity region are governed by Laplace equations as [39]:

$$\nabla^2 T_p = 0, \quad \rho < a, \tag{2}$$

$$\nabla^2 T = 0, \quad a < \rho < b, \tag{3}$$

$$\nabla^2 T_w = 0, \quad \rho > b. \tag{4}$$

The applicable boundary conditions at the particle's surface and cavity wall are the temperature jump and continuity of normal heat flux [39]:

$$T_p \text{ is finite} : \rho < a, \tag{5}$$

$$T - T_p = C_t \, l \, \frac{\partial T}{\partial \rho}, \quad \rho = a, \tag{6}$$

$$k_A \frac{\partial T}{\partial \rho} = k_p \frac{\partial T_p}{\partial \rho}, \quad \rho = a, \tag{7}$$

$$T - T_w = -C_t' \, l \frac{\partial T}{\partial \rho}, \quad \rho = b, \tag{8}$$

$$k_A \frac{\partial T}{\partial \rho} = k_w \frac{\partial T_w}{\partial \rho}, \quad \rho = b, \tag{9}$$

also, far from cavity wall surface condition $\rho \to \infty$ is given as:

$$T_w \to T_\infty = T_0 - E_\infty \, \rho \, \cos\theta, \quad \rho > b, \tag{10}$$

where C_t' is temperature jump coefficient at cavity wall surface.
Temperature distributions for all regions are given by

$$T_p = T_0 - 2 \, A \, E_\infty \, \rho \, \cos\theta, \quad \rho < a, \tag{11}$$

$$T = T_0 - E_\infty \left[A \, Y + A \, X \left(\frac{a}{\rho} \right)^2 \right] \rho \, \cos\theta, \quad a < \rho < b, \tag{12}$$

$$T_w = T_0 - E_\infty \left[1 - A \, B \left(\frac{b}{\rho} \right)^2 \right] \rho \, \cos\theta, \quad \rho > b, \tag{13}$$

where

$$A = 2 \, k_w^* \, \left[(1 + k_w^* + k_w^* \, \tilde{C}_t') \, Y - (1 - k_w^* + k_w^* \, \tilde{C}_t') \, X \, \lambda^2 \right]^{-1},$$

$$B = \left[(k_w^* \, \tilde{C}_t' + k_w^* - 1) \, Y - (k_w^* \, \tilde{C}_t' - k_w^* - 1) \, X \, \lambda^2 \right] \, (2 \, k_w^*)^{-1},$$

$$X = 1 - k_p^* + k_p^* \, \tilde{C}_t, \; Y = 1 + k_p^* + k_p^* \, \tilde{C}_t,$$

$$\tilde{C}_t = C_t \, l/a, \; \tilde{C}_t' = C_t' \, l/b, \lambda = a/b, \; k_p^* = k_p/k_A, \; k_w^* = k_p/k_A.$$

2.2. Velocity distributions

The continuity and momentum equations under the Stokesian assumptions of Brinkman fluid without body forces are given by [32, 33, 40]:

$$\nabla \cdot \vec{u} = 0, \tag{14}$$

$$\nabla p + \tilde{\mu} \, \nabla^2 \vec{u} + \frac{\mu}{k_1} \, \vec{u} = 0. \tag{15}$$

In Eqs. (14) and (15), $\vec{u}$, p, μ represent the velocity vector, pressure, and viscosity of the fluid, respectively. $\tilde{\mu}$ is effective viscosity and k_1 is the permeability of porous medium. The expression for stress tensor t_{ij} can be expressed as:

$$t_{ij} = -p\, I + 2\,\tilde{\mu}\,\Delta. \tag{16}$$

Here $\Delta = \dfrac{1}{2}\left(\nabla\vec{u} + (\nabla\vec{u})^t\right)$, and $(\nabla\vec{u})^t$ is the transpose of $\nabla\,\vec{u}$, and I is unit dyadic.

Since the problem is two-dimensional, so we have supposed components of the velocity vector as

$$\vec{u}(\rho,\,\theta) = u_\rho\,\vec{e}_\rho + u_\theta\,\vec{e}_\theta. \tag{17}$$

Furthermore, the axisymmetric motion plays a crucial role for defining the velocity components in terms of the stream function ψ as:

$$u_\rho = \frac{1}{\rho}\frac{\partial\psi}{\partial\theta} \quad \text{and} \quad u_\theta = -\frac{\partial\psi}{\partial\rho}. \tag{18}$$

Introducing nondimensional parameters $\rho = b\,\tilde{\rho}$, $u = U\,\tilde{u}$, $p = (\tilde{\mu}\,U\,p/b)$, $\nabla = (\tilde{\nabla}/b)$ [32], into Eq. (15) and dropping the tildes, we get the reduced equations as

$$\frac{\partial p}{\partial\rho} = \frac{\tilde{\mu}}{\rho}\frac{\partial}{\partial\theta}\left(\nabla^2 - \alpha^2\right)\psi, \tag{19a}$$

$$\frac{\partial p}{\partial\theta} = -\tilde{\mu}\rho\frac{\partial}{\partial\rho}\left(\nabla^2 - \alpha^2\right)\psi, \tag{19b}$$

where

$$\nabla^2 = \frac{\partial^2}{\partial\rho^2} + \frac{1}{\rho}\frac{\partial}{\partial\rho} + \frac{1}{\rho^2}\frac{\partial^2}{\partial\theta^2} \text{ is Laplacian operator and } \alpha = \sqrt{\frac{\mu b^2}{\tilde{\mu}k_1}}$$

is the permeability parameter.

From Eq. (19), we have obtained the pressure term

$$p = \tilde{\mu}\,\alpha^2\left(\frac{P}{\rho} - Q\,\rho\right)\cos\theta. \tag{20}$$

Eliminating pressure from Eq. (19), we have obtained the following equation satisfied by the stream function given as:

$$\nabla^2\left(\nabla^2 - \alpha^2\right)\psi = 0. \tag{21}$$

The solution of Eq.(21) is given by [41]

$$\psi = \left[\frac{P}{\rho} + Q\,\rho + R\,I_1(\alpha\,\rho) + S\,K_1(\alpha\,\rho)\right]\sin\theta, \tag{22}$$

where $I_1(\alpha\,\rho)$ and $K_1(\alpha\,\rho)$ are the modified Bessel's functions of first and second kind of order 1, respectively. The expressions for velocity components, normal stress $t_{\rho\rho}$ and shear stress $t_{\rho\theta}$ are given as:

$$u_\rho = \left[\frac{P}{\rho^2} + Q + \frac{R}{\rho}\,I_1(\alpha\,\rho) + \frac{S}{\rho}\,K_1(\alpha\,\rho)\right]\cos\theta, \tag{23}$$

$$u_\theta = \left[\frac{P}{\rho^2} - Q + \frac{R}{\rho}\,(I_1(\alpha\,\rho) - \alpha\,\rho\,I_0(\alpha\,\rho)) + \frac{S}{\rho}\,(K_1(\alpha\,\rho) + \alpha\,\rho\,K_0(\alpha\,\rho))\right]\sin\theta, \tag{24}$$

$$t_{\rho\rho} = -\tilde{\mu}\left[\frac{P}{\rho^3}(4+\alpha^2\rho^2) - Q\alpha^2\rho + \frac{R}{\rho^2}\,(4I_1(\alpha\rho) - 2\alpha\rho I_0(\alpha\rho)) + \frac{S}{\rho^2}\,(4K_1(\alpha\rho) + 2\alpha\rho K_0(\alpha\rho))\right]\cos\theta, \tag{25}$$

$$t_{\rho\,\theta} = -\tilde{\mu}\left[\frac{4\,P}{\rho^3} + \frac{R}{\rho^2}\left((4+\alpha^2\,\rho^2)\,I_1(\alpha\,\rho) - 2\,\alpha\,\rho\,I_0(\alpha\,\rho)\right) + \frac{S}{\rho^2}\left((4+\alpha^2\,\rho^2)\,K_1(\alpha\,\rho) + 2\,\alpha\,\rho\,K_0(\alpha\,\rho)\right)\right]\sin\theta, \tag{26}$$

where $I_0(\alpha\,\rho)$ and $K_0(\alpha\,\rho)$ are the modified Bessel's functions of first and second kind of order 0, respectively.

To find the arbitrary constants P, Q, R, and S, we have to apply hydrodynamic slip boundary conditions at the surface of particle and cavity wall as [36, 39]

$$u_\rho = U\,\cos\theta, \quad \rho = a, \tag{27}$$

$$u_\theta = -U\sin\theta + \frac{C_m\,l}{\tilde{\mu}}\,t_{\rho\,\theta} + \frac{C_s\,\tilde{\mu}}{\rho_A\,T_0}\,\frac{1}{\rho}\,\frac{\partial T}{\partial\theta} - \frac{C_m\,l\,C_h\,\tilde{\mu}}{\rho_A\,T_0}\,\frac{\partial}{\partial\,\rho}\left(\frac{1}{\rho}\,\frac{\partial T}{\partial\,\theta}\right), \quad \rho = a, \tag{28}$$

$$u_\rho = 0, \quad \rho = b, \tag{29}$$

$$u_\theta = -\frac{C'_m\,l}{\tilde{\mu}}\,t_{\rho\,\theta} + \frac{C'_s\,\tilde{\mu}}{\rho_A\,T_0}\,\frac{1}{\rho}\,\frac{\partial T}{\partial\theta} + \frac{C'_m\,l\,C'_h\,\tilde{\mu}}{\rho_A\,T_0}\,\frac{\partial}{\partial\,\rho}\left(\frac{1}{\rho}\,\frac{\partial T}{\partial\,\theta}\right), \quad \rho = b, \tag{30}$$

where C'_m, C'_s, C'_h are frictional slip, thermal creep and thermal stress slip, respectively, at cavity wall. ρ_A denotes the density of the medium.

By substituting Eqs.(11)–(13) and Eqs. (23)–(26) in the boundary conditions (27)–(30), we get the following system of linear equations as

$$P + Q\,\lambda^2 + R\lambda\,I_1(\alpha\,\lambda) + S\,\lambda\,K_1(\alpha\,\lambda) = U\,\lambda^2, \tag{31}$$

$$P\,\sigma_1 + R\,\left[\lambda\, I_1(\alpha\lambda)\,\sigma_2 - \alpha\,\lambda^2\,\sigma_3\, I_0(\alpha\lambda)\right] + S\,\left[\lambda\, K_1(\alpha\lambda)\,\sigma_2 + \alpha\,\lambda^2\,\sigma_3\, K_0(\alpha\lambda)\right] - Q\,\lambda^2 = -U\,\lambda^2 + 2\,\tilde{C_m}\,C_h\,\delta\,A\,X\,\lambda^2 + C_s\,\delta\,A\,(Y+X)\,\lambda^2, \quad (32)$$

$$P + Q + R\,I_1(\alpha) + S\,K_1(\alpha) = 0, \quad (33)$$

$$P\,\sigma_4 - Q + R\,\left[I_1(\alpha)\,\sigma_5 - \alpha\,\sigma_6\, I_0(\alpha)\right] + S\,\left[K_1(\alpha)\,\sigma_5 + \alpha\,\sigma_6\, K_0(\alpha)\right] = -2\,\tilde{C_m'}\,C_h'\,\delta\,A\,X\,\lambda^2 + C_s'\,\delta\,A\,(Y + X\,\lambda^2), \quad (34)$$

where $\delta = \dfrac{\tilde{\mu}\,E_\infty}{\rho_A\,T_0}$, and $\sigma_j; 1 \leqslant j \leqslant 6$ have shown in Appendix section. The expressions for P, Q, R, and S are very lengthy and cumbersome. So, they are not given in the paper.

2.3. Thermophoretic mobility in the medium

The drag force exerted on inner rigid cylinder immersed in a bounded porous medium is given by [42, 43]

$$F_T = \int_0^{2\,\pi} \left[\rho(t_{\rho\,\rho}\,\cos\theta - t_{\rho\,\theta}\,\sin\theta)\right]_{\rho=\lambda}\,d\,\theta. \quad (35)$$

Here

$$t_{\rho\,\rho} = -p + 2\,\tilde{\mu}\,\frac{\partial\,u_\rho}{\partial\,\rho}. \quad (36)$$

Inserting the values of $t_{\rho\,\rho}$ and $t_{\rho\,\theta}$, we obtained the drag force on inner cylinder

$$F_T = -\tilde{\mu}\,\pi\,\lambda\,\alpha^2\left[P\,\lambda^{-1} - Q\,\lambda - R\,I_1(\alpha\lambda) - S\,K_1(\alpha\lambda)\right]. \quad (37)$$

Since the particle remains suspended freely in the porous medium, the force F_T must be zero, therefore

$$P\,\lambda^{-1} - Q\,\lambda - R\,I_1(\alpha\lambda) - S\,K_1(\alpha\lambda) = 0. \quad (38)$$

Now, substituting P, Q, R, S in Eq.(38) yields the thermophoretic velocity of the particle in the form

$$U_T = U_{os} + M_T\,U_0. \quad (39)$$

Furthermore, when $C_h' = C_m' = C_s' = 0$ at cavity surface and $M_T \to 1$, then $U_T \to U_0$, *i.e.*, the thermophoretic velocity in absence of porous medium as

$$U_0 = \frac{\mu E_\infty}{\rho_A T_0}\,\frac{C_s\,(Y+X) + 2\,\tilde{C_m}\,C_h\,X}{Y\,(1 + 2\,\tilde{C_m})}, \quad (40)$$

which is thermophoretic velocity of the corresponding unbounded cylindrical particle the same as Eq.(1), and

$$U_{os} = 2\,\frac{\delta\,\Omega_2\,A}{\gamma}\,[C_s'\,(Y + X\,\lambda^2) - 2\,\tilde{C_m'}\,C_h'\,X\,\lambda^2]. \tag{41}$$

Here, the thermoosmotic velocity U_{os} indicates the translational velocity rising from the interaction between thermal creep at the cavity wall and prescribed temperature gradient, *i.e.*, there is no thermophoretic motion ($C_h = C_s = 0$). Also

$$U_{os}^{*} = \frac{U_{os}}{C_s'\,\delta}, \tag{42}$$

which represents the nondimensionalized thermoosmosis velocity along the cavity wall and

$$M_T = \frac{P\,(1 + 2\,\tilde{C_m})\,A\,\Omega_1}{\gamma} \tag{43}$$

denotes the dimensionless thermophoretic mobility of the particle, which is independent of thermal creep parameters (C_s, C_s').

2.3.1. Bounded medium

In absence of porous medium, *i.e.*, $k_1 \to \infty$ thermophoretic velocity of the particle in cylindrical cavity is given as

$$U_T = \frac{\mu E_\infty}{\rho_A T_0}\,\frac{A\,\left[X\,\left((C_s + \tilde{C}_m C_h)\sigma_6 - (C_s' - 2\tilde{C'}_m C_h')\,\sigma_3\lambda^2\right) - Y(C_s'\sigma_3 - C_s\sigma_6)\right]}{2\,\sigma_3\,\sigma_6}, \tag{44}$$

where $\Omega_i; i = 1, 2, \gamma$, $\sigma_j; 1 \leqslant j \leqslant 8$, $\tau_k; 1 \leqslant k \leqslant 5$ have shown in the Appendix section.

2.3.2. Unbounded medium

As $\lambda \to 0$, and when thermal conductivity at cavity wall surface $k_w \to k_A$, we have obtained the following cases:

Case I: Thermophoretic velocity of the cylindrical particle in Brinkman medium is given as

$$U_T = \frac{4\,\delta\,\left(C_s\,(Y + X) + 2\,\tilde{C_m}\,C_h\,X\right)\,K_1(\alpha)}{\left[(\tilde{C_m}\alpha^2 + 4\,(1 + 2\,\tilde{C_m}))K_1(\alpha) + \alpha(1 + 2\tilde{C_m})K_0(\alpha)\right]\,Y}, \tag{45}$$

which is the same as the result of Faltas and Ragab [36].

Case II: In absence of porous medium, thermophoretic velocity of the particle is given as

$$U_T = \frac{\mu E_\infty}{\rho_A T_0}\,\frac{\left(C_s\,(Y + X) + 2\,\tilde{C_m}\,C_h\,X\right)}{2(1 + 2\,\tilde{C_m})\,Y}, \tag{46}$$

which shows a good agreement with the expression obtained by Chang and Keh [18].

Case III: In absence of thermal stress slip parameter $C_h \to 0$, Eq. (46) reduces to

$$U_T = \frac{\mu E_\infty}{\rho_A T_0} \frac{C_s\,(Y+X)}{2(1+2\,\tilde{C_m})\,Y}, \tag{47}$$

which shows a good agreement with the expression obtained by Keh and Tu [13].

3. Analysis of results

In this analysis, we have considered the thermal properties and slip parameters at particle and cavity surfaces are the same; $i.e., k_p^* = k_w^*(k_p = k_w)$, $\tilde{C_t'} = \lambda\,\tilde{C_t}(C_t' = C_t)$, $\tilde{C_m'} = \lambda\,\tilde{C_m}(C_m' = C_m)$, $C_s' = C_s$, $C_h' = C_h$, and $\tilde{\mu} = \mu$ recommended in refs. [27, 32, 39]. Talbot et al. [44] suggested a set of kinetic theory values for temperature jump and slip coefficients as $C_t = 2.28, C_m = 1.14, C_s = 1.17$. We have found the expressions for temperature distributions, thermoosmotic velocity, thermophoretic mobility and normalized velocity, and presented graphically and interpreted them. The thermophoretic mobilities and net normalized velocity depends upon the various parameters:

1. The permeability ($0 \leqslant k_1 \leqslant \infty$) [36, 39].
2. The thermal conductivity ratio of particle to overall thermal conductivity of the porous medium($0 \leqslant k_p^* < \infty$) [27, 39].
3. The frictional / viscous slip parameter ($0 \leqslant \tilde{C_m} < \infty$) [25, 27, 39].
4. The ratio of the particle-to-cavity radii ($0.01 \leqslant \lambda \leqslant 1$) [27, 39].
5. The ratio of thermal stress slip to thermal creep parameters ($0 \leqslant C_h/C_s < \infty$) [39].

The normalized thermoosmotic velocity U_{os}^* of the confined inner cylinder caused by the circulation of thermoosmotic flow along a cavity wall. The expression for U_{os}^* is presented in Eq. (42), and graphs are shown in Figs. 2–5 to examine the impact of the permeability, thermal conductivity ratio of particle to medium, frictional slip parameter, and radii ratio of particle to cavity. Figs. 2 and 3 depicts the variation of thermoosmotic velocity versus the permeability for various values of the particle's thermal conductivity ratio and frictional slip parameter. We have observed that U_{os}^* sharply increases with an increase in permeability. Also, it is noticed that thermoosmotic velocity increases when the thermal conductivity of particle or thermal conductivity ratio of particle to medium increases. Because the lower permeability denotes the frictional forces being larger than inertial forces, this suggests the medium is more porous. Hence, the thermoosmotic velocity of particle declines for low parmeability. However, the high permeability denotes reduced frictional forces. So that velocity of cylindrical particle grows as permeability rises. In Fig. 3, we have observed the enhancement of velocity with an increase in

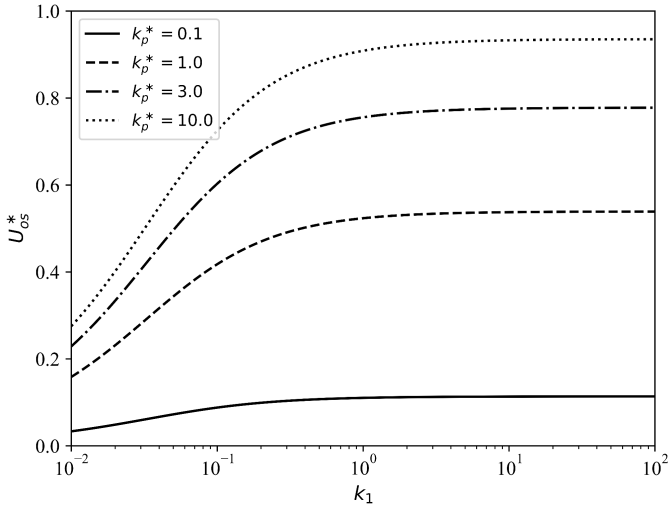

Fig. 2. Plots of U_{os}^* versus k_1 when $\lambda = 0.3$, $C_h' = 1$, $\tilde{C}_m = 0.1$, $\tilde{C}_t = 0.2$

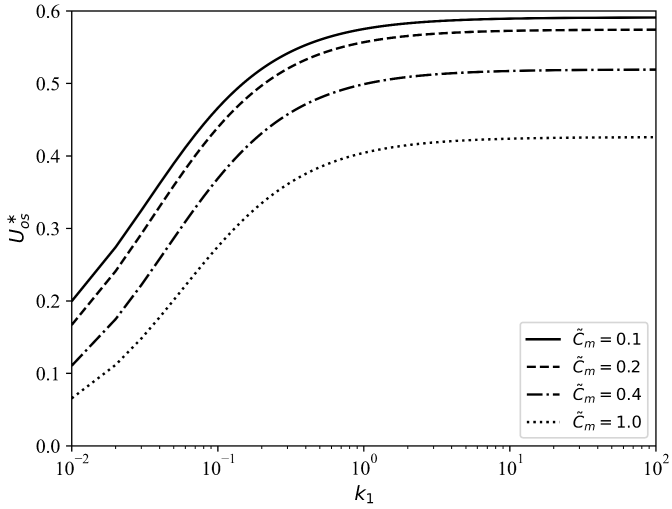

Fig. 3. Plots of U_{os}^* versus k_1 when $k_p^* = k_w^* = 1, \lambda = 0.25$, $C_h' = 1$, $\tilde{C}_t = 0.2$

permeability, also it is noticed that it shows more effect for low value of frictional slip parameter.

Figs. 4 and 5 represents the variation of thermoosmotic velocity versus the radii ratio for various values of frictional slip parameter and permeability. The impact of frictional slip and permeability on U_{os}^* declines when $\lambda \to 1$. The value of U_{os}^* decreases with increase in $\tilde{C}_m$, while the value of U_{os}^* increases with increase in k_1, and shows its extreme value at $\lambda = 0.01$. Increasing the radii ratio means that

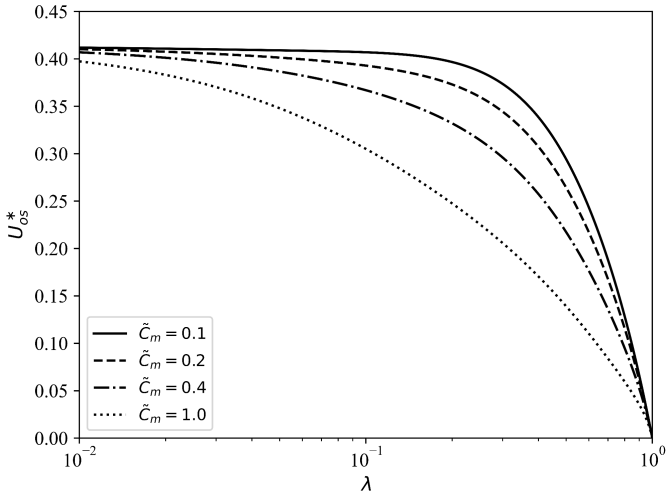

Fig. 4. Plots of U^*_{os} versus λ when $k^*_p = k^*_w = 1$, $C'_h = 1$, $k_1 = 0.06$, $\tilde{C}_t = 0.2$

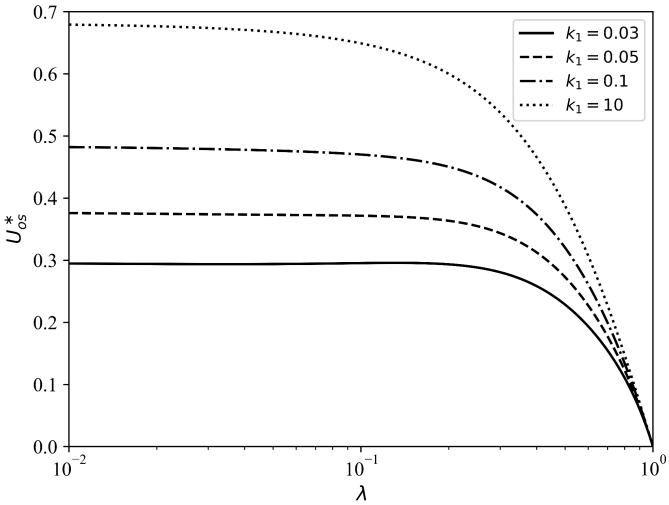

Fig. 5. Plots of U^*_{os} versus λ when $k^*_p = k^*_w = 1$, $C'_h = 1$, $\tilde{C}_m = 0.1$, $\tilde{C}_t = 0.2$

the particle approaches to the cavity wall, due to this reason, the movement of the particle becomes slow, i.e., thermoosmotic velocity decreases as $\lambda \to 1$.

The normalized mobility constant M_T of a cylindrical particle in a cavity is described by Eq. (43). The thermophoretic mobility is independent of thermal creep and thermal stress slip at the cavity surface ($C'_s = C'_h = 0$). The variation of mobility constant is shown in Figs. 6–8. Here, Fig. 6 illustrates the same behavior as Fig. 2, and attains maximum value for the case of clear fluid ($k_1 \geqslant 100$). The mobility constant slightly increases as k_1 increases, and $M_T \to 0$ for lower value of the permeability or $k_1 \to 0$. In Fig. 7, there is seen an increasing effect in mobility

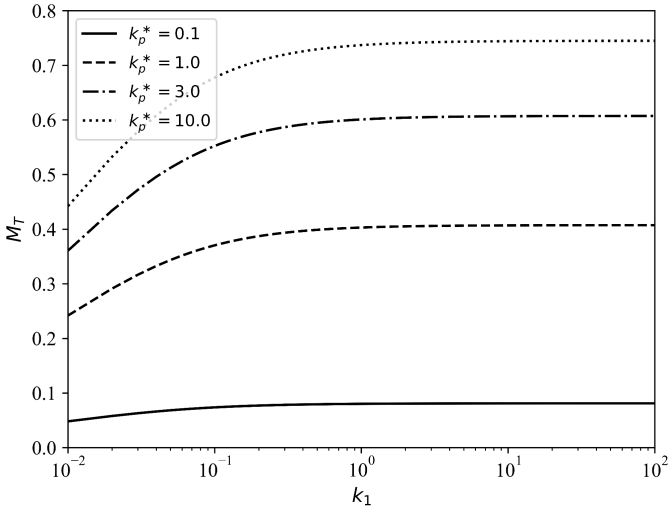

Fig. 6. Plots of M_T versus k_1 when $\lambda = 0.3$, $\tilde{C}_m = 0.1$, $\tilde{C}_t = 0.2$

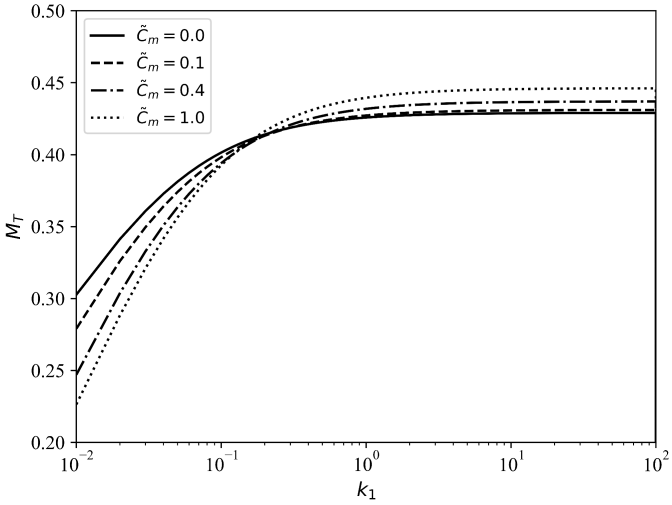

Fig. 7. Plots of M_T versus k_1 when $k_p^* = k_w^* = 1, \lambda = 0.25$, $C_h' = 1$, $\tilde{C}_t = 0.2$

constant with increasing in permeability. Here, it is interesting to note that M_T shows maxiumum variation for lowest frictional slip parameter ($\tilde{C}_m = 0.0$) in the range of permeability between 10^{-2} and 0.2. However, when $0.2 < k_1 < 10^2$, we have found reverse effect (curve of M_T maximum for $\tilde{C}_m = 1.0$). Fig. 8 shows that M_T decreases with increasing radii ratio of particle to cavity, and decreasing thermal conductivity ratio of particle to medium. M_T attains its maximum value when $\lambda = 0.01$, while M_T slightly downs as $\lambda \to 1$. We have observed that thermoosmotic velocity and

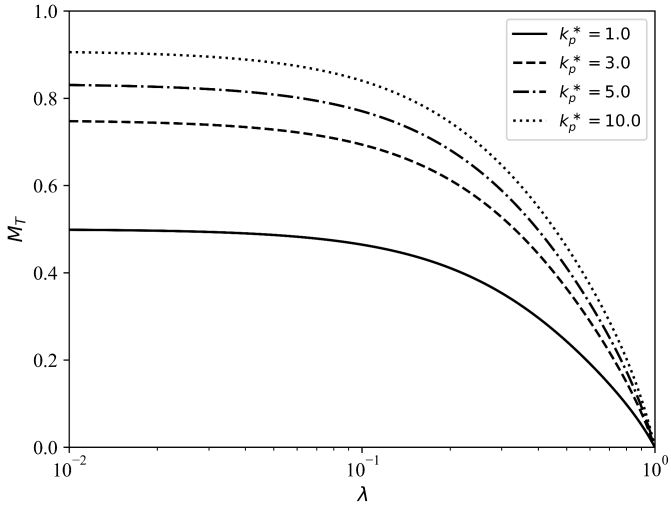

Fig. 8. Plots of M_T versus λ when $k_1 = 0.06$, $\tilde{C}_m = 0.1$, $\tilde{C}_t = 0.2$

thermophoretic mobility of the particle are a decreasing function of radii ratio, while increasing function of permeability, and thermal conductivity ratio.

The normalized thermophoretic velocity U_T/U_0 is the ratio of velocity in bounded and unbounded medium. The velocity U_T/U_0 of a cylindrical particle at $C_s = C_s'$ and $C_h = C_h'$ is caused by a uniform temperature gradient. The expression of net normalized velocity obtained from Eqs. (39) and (40) as a function of relevant parameters, are presented graphically in Figs. 9–12. In Figs. 9–10, we have observed that U_T/U_0 increases with an increase in the permeability. It also represents the maximum value of net normalized velocity for the higher values

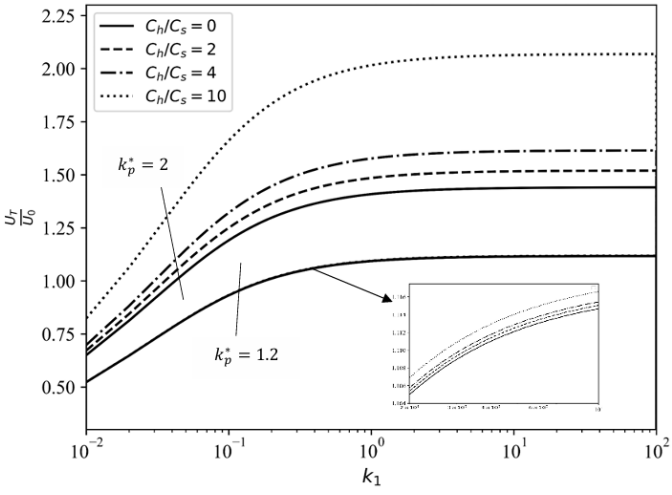

Fig. 9. Plots of U_T/U_0 versus k_1 when $\lambda = 0.2$, $\tilde{C}_m = 0.1$, $\tilde{C}_t = 0.2$

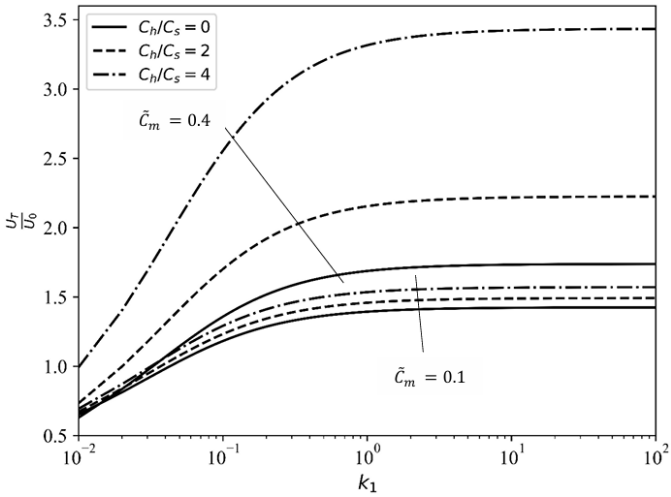

Fig. 10. Plots of U_T/U_0 versus k_1 when $\lambda = 0.2, k_w^* = k_p^* = 2, \tilde{C}_m = 0.1, \tilde{C}_t = 0.2$

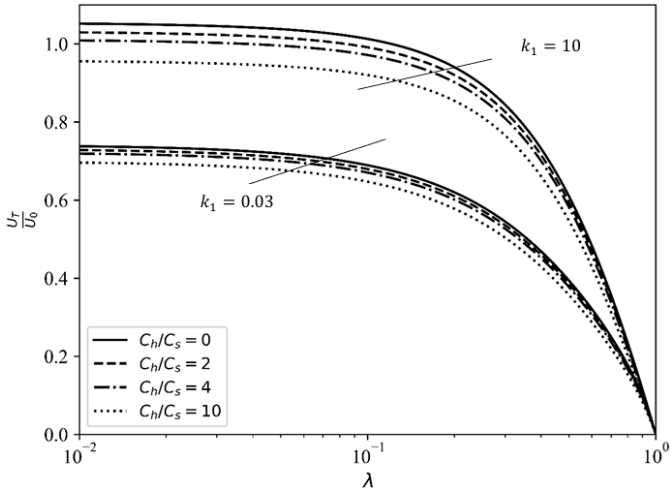

Fig. 11. Plots of U_T/U_0 versus λ when $k_p^* = k_w^* = 1,\ \tilde{C}_m = 0.1,\ \tilde{C}_t = 0.2$

of the thermal conductivity ratio parameter, viscous slip parameter and the ratio of thermal stress slip and thermal creep coefficients. In both Figs.9–10, we have observed the net normalized velocity increases as permeability rises. This happens because high permeability medium behaves like a clear fluid, so that velocity increases as $k_1 \to \infty$. Variation of U_T/U_0 versus the radii ratio for various values of permeability, viscous slip parameter, and ratio of thermal stress slip and thermal creep are presented in Figs. 11 and 12. Usually, as increase in radii ratio of particle to cavity, net normalized velocity decreases due to decrease in the gap between particle and cavity. In Fig. 11, we have found that U_T/U_0 attains its maximum

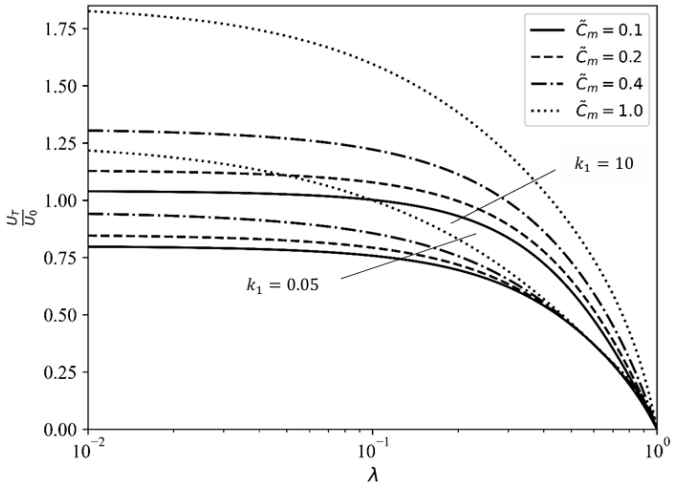

Fig. 12. Plots of U_T/U_0 versus λ when $k_p^* = k_w^* = 1, C_h = 0, \tilde{C}_t = 0.2$

value for the lower value of C_h/C_s and higher value of k_1. Fig. 12 presents, for the whole range of radii ratio and given values of the permeability, U_T/U_0 grows as and frictional slip parameter rises.

4. Conclusions

This paper examines analytically the thermophoretic motion of rigid cylinder located concentrically within a cylindrical cavity. This investigation is conducted with the consideration of negligible Reynolds and Péclet numbers. During this analysis, we applied the temperature jump, viscous slip, thermal creep, and thermal stress slip at the particle and cavity wall surface. Analytical expressions for thermoosmotic velocity, thermophoretic mobility and net normalized velocity of a cylindrical particle are obtained. The main results are as follows:

- The thermoosmotic velocity, thermophoretic mobility and normalized velocity show increasing effect with an increase in permeability.
- We have observed that for whole range of radii ratio, thermoosmotic velocity, mobility constant and net normalized velocity decrease, and approach 0 when radii ratio is 1.
- The thermoosmotic velocity and mobility constant are monotonically increasing function of thermal conductivity ratio.
- The normalized thermophoretic velocity represents maximum effect for higher value of thermal conductivity ratio, viscous slip parameter and permeability.
- The thermoosmotic velocity, thermophoretic mobility and normalized velocity have maximum value in absence of the cavity.

- The effect of ratio of thermal stress slip parameter and thermal creep parameter enhance or reduce the net normalized velocity, depending upon the characteristics of particle and medium.

Our results are matched with the previous published results available in the literature for the cases of absence of cavity wall, porous medium and thermal stress slip parameter. Also, we have obtained the expression for thermophoretic velocity of cylindrical particle in bounded viscous fluid. The boundary effect on the thermophoretic motion of a particle in a porous medium can be significant. Various problems such as thermophoresis of cylindrical particle parallel to its axis, and a particle in micropolar fluid are considered as future aspects.

Appendix

The expressions mentioned in Eqs.(32), (34), (41), and (43) are given as

$$\Omega_1 = \tau_4\,\alpha\,\lambda\,\sigma_6 + \tau_1 - \tau_2\,\alpha\,\sigma_6 + \tau_1\,\sigma_5,\ \Omega_2 = \tau_3\,\alpha\,\sigma_3 - \tau_1 - \tau_1\,\sigma_2 - \tau_5\,\alpha\,\lambda\,\sigma_3,$$

$$\gamma = \Big[\alpha\,\sigma_3\ (\sigma_5\,\tau_4 - \sigma_4\,\tau_4 - \alpha\,\tau_1\,\sigma_6)\,\lambda^3 + (\alpha\,\sigma_3\,\tau_6\,(\tau_4+1) + (\tau_2+1)\,\sigma_7)\,\lambda^2 \left(\alpha\,\sigma_3\,\tau_4\,(\sigma_5+1) + \alpha\,\sigma_6\,\tau_3\,(\sigma_1+1) - \alpha^2\,\sigma_3\,\sigma_6\,\tau_1\right)\,\lambda - (\sigma_1+\sigma_2+2)\,\sigma_8\Big],$$

$$\sigma_1 = 1 + 4\,\tilde{C}_m,\ \sigma_2 = 1 + 4\,\tilde{C}_m + \tilde{C}_m\,\alpha^2\,\lambda^2,\ \sigma_3 = 1 + 2\,\tilde{C}_m,\ \sigma_4 = 1 - 4\,\tilde{C'}_m,$$

$$\sigma_5 = 1 - 4\,\tilde{C'_m} - \tilde{C'_m}\,\alpha^2,\ \sigma_6 = 1 - 2\,\tilde{C'_m},\ \sigma_7 = (\sigma_4\,\tau_5 - \sigma_5\,\tau_5 - \alpha\,\tau_2\,\sigma_6),$$

$$\sigma_8 = (\tau_5 + \alpha\,\tau_2\,\sigma_6 + \sigma_5\,\tau_5),\ \tau_1 = K_1(\alpha\,\lambda)\,I_1(\alpha) - I_1(\alpha\,\lambda)\,K_1(\alpha),$$

$$\tau_2 = K_1(\alpha\,\lambda)\,I_0(\alpha) + I_1(\alpha\,\lambda)\,K_0(\alpha),\ \tau_3 = K_1(\alpha\,\lambda)\,I_0(\alpha\,\lambda) + I_1(\alpha\,\lambda)\,K_0(\alpha\,\lambda),$$

$$\tau_4 = K_1(\alpha)\,I_0(\alpha) + I_1(\alpha)\,K_0(\alpha),\ \tau_5 = I_0(\alpha\,\lambda)\,K_1(\alpha) + K_0(\alpha\,\lambda)\,I_1(\alpha).$$

Acknowledgements

The first author, Shekhar Nishad, is highly thankful to the institute research fellowship of the National Institute of Technology, Raipur.

References

[1] V.G. Chernyak and T.V. Sograbi. The role of boundary conditions in the theory of aerosol particle thermophoresis. *Physics of Fluids*, 35(10):107128, 2023. doi: 10.1063/5.0173266.

[2] E.H. Kennard et al. *Kinetic Theory of Gases*. McGraw-hill, 1938.

[3] Y.Ye, D.Y.H. Pui, B.Y.H. Liu, S. Opiolka, S. Blumhorst, and H. Fissan. Thermophoretic effect of particle deposition on a free standing semiconductor wafer in a clean room. *Journal of Aerosol Science*, 22(1):63–72, 1991. doi: 10.1016/0021-8502(91)90093-W.

[4] M.M.R. Williams and S.K. Loyalka. *Aerosol Science: Theory and Practice*. Pergamon Press, 1991.

[5] S.K. Friedlander et al. *Smoke, Dust, and Haze*. Oxford University Press, 2000.

[6] A.G.B.M. Sasse, W.W. Nazaroff, and A.J. Gadgil. Particle filter based on thermophoretic deposition from natural convection flow. *Aerosol Science and Technology*, 20(3):227–238, 1994. doi: 10.1080/02786829408959679.

[7] W. Liu, J. Cui, J. Wang, G. Xia, and Z. Li. Negative thermophoresis of nanoparticles in liquids. *Physics of Fluids*, 35(3):032004, 2023. doi: 10.1063/5.0133385.

[8] F. Zheng. Thermophoresis of spherical and non-spherical particles: a review of theories and experiments. *Advances in Colloid and Interface Science*, 97(1-3):255–278, 2002. doi: 10.1016/S0001-8686(01)00067-7.

[9] J.R. Brock. On the theory of thermal forces acting on aerosol particles. *Journal of Colloid Science*, 17(8):768–780, 1962. doi: 10.1016/0095-8522(62)90051-X.

[10] K.H. Leong. Thermophoresis and diffusiophoresis of large aerosol particles of different shapes. *Journal of Aerosol Science*, 15(4):511–517, 1984. doi: 10.1016/0021-8502(84)90047-8.

[11] Y.C. Chang and H.J. Keh. Thermophoretic motion of slightly deformed aerosol spheres. *Journal of Aerosol Science*, 41(2):180–197, 2010. doi: 10.1016/j.jaerosci.2009.10.004.

[12] E. Maghsoudi, M.J. Martin, and R. Devireddy. Momentum and heat transfer in laminar slip flow over a cylinder. *Journal of thermophysics and heat transfer*, 27(4):607–614, 2013. doi: 10.2514/1.T3997.

[13] H.J. Keh and H.J. Tu. Thermophoresis and photophoresis of cylindrical particles. *Colloids and Surfaces A: Physicochemical and Engineering Aspects*, 176(2-3):213–223, 2001. doi: 10.1016/S0927-7757(00)00567-7.

[14] Y. Sone. A flow induced by thermal stress in rarefied gas. *Journal of the Physical Society of Japan*, 33(1):232–236, 1972. doi: 10.1143/JPSJ.33.232.

[15] D.A. Lockerby, J.M. Reese, D.R. Emerson, and R.W. Barber. Velocity boundary condition at solid walls in rarefied gas calculations. *Physical Review E*, 70(1):017303, 2004. doi: 10.1103/PhysRevE.70.017303.

[16] Y.C. Chang and H.J. Keh. Effects of thermal stress slip on thermophoresis and photophoresis. *Journal of Aerosol Science*, 50:1–10, 2012. doi: 10.1016/j.jaerosci.2012.03.006.

[17] D.W. Mackowski. Photophoresis of aerosol particles in the free molecular and slip-flow regimes. *International Journal of Heat and Mass Transfer*, 32(5):843–854, 1989. doi: 10.1016/0017-9310(89)90233-0.

[18] Y.C. Chang and H.J. Keh. Thermophoresis and photophoresis of an aerosol cylinder with thermal stress slip. *American Journal of Heat and Mass Transfer*, 4(2):85–103, 2017.

[19] Y.M. Tseng and H.J. Keh. Thermophoresis of a cylindrical particle at small finite péclet numbers. *Aerosol Science and Technology*, 55(1):54–62, 2021. doi: 10.1080/02786826.2020.1812504.

[20] V.B. Dung. General thermophoretic force on a small spherical particle in gases. *Indian Journal of Physics*, 98:4505–4513, 2024. doi: 10.1007/s12648-024-03201-8.

[21] M.N. Bashir, A. Rauf, S.A. Shehzad, M. Ali, and T. Mushtaq. Thermophoresis phenomenon in radiative flow about vertical movement of a rotating disk in porous region. *Advances in Mechanical Engineering*, 14(7):1–14, 2022. doi: 10.1177/16878132221115019.

[22] M.M. Bhatti, M.A. Abbas, and S. Muhammad. Optimizing fluid flow efficiency: third-grade hybrid nanofluid flow with electro-magneto-hydrodynamics in confined vertical spaces. In *Nanofluids*, pages 243–275. 2024. doi: 10.1016/B978-0-443-13625-2.00012-7.

[23] P. Sarkar and K.P. Madasu. Parallel and perpendicular flows of a couple stress fluid past a solid cylinder in cell model: Slip condition. *Physics of Fluids*, 35(3):033101, 2023. doi: 10.1063/5.0135866.

[24] M. Marin, A. Öchsner, and M.M. Bhatti. Some results in moore-gibson-thompson thermoelasticity of dipolar bodies. *ZAMM-Journal of Applied Mathematics and Mechanics/Zeitschrift für Angewandte Mathematik und Mechanik*, 100(12):e202000090, 2020. doi: 10.1002/zamm.202000090.

[25] H.J. Keh and J.H. Chang. Boundary effects on the creeping-flow and thermophoretic motions of an aerosol particle in a spherical cavity. *Chemical Engineering Science*, 53(13):2365–2377, 1998. doi: 10.1016/S0009-2509(98)00066-9.

[26] H.J. Keh and N.Y. Ho. Concentration effects on the thermophoresis of aerosol spheres. *Journal of Colloid and Interface Science*, 216(1):167–178, 1999. doi: 10.1006/jcis.1999.6310.

[27] C.Y. Li and H.J. Keh. Thermophoresis of a particle in a concentric cavity with thermal stress slip. *Aerosol Science and Technology*, 52(3):269–276, 2018. doi: 0.1080/02786826.2017.1398397.

[28] C.Y. Li and H.J. Keh. Axisymmetric thermophoresis of an aerosol particle in a spherical cavity. *Journal of Aerosol Science*, 135:33–45, 2019. doi: 10.1016/j.jaerosci.2019.05.002.

[29] Y.M. Tseng and H.J. Keh. Thermophoretic motion of an aerosol sphere in a spherical cavity. *European Journal of Mechanics - B/Fluids*, 81:93–104, 2020. doi: 10.1016/j.euromechflu.2019.12.010.

[30] N.A. Shah, S.J. Yook, and O. Tosin. Analytic simulation of thermophoretic second grade fluid flow past a vertical surface with variable fluid characteristics and convective heating. *Scientific Reports*, 12(1):5445, 2022. doi: 10.1038/s41598-022-09301-x.

[31] M. Sarfraz, M. Khan, and A. Ahmed. Study of thermophoresis and brownian motion phenomena in radial stagnation flow over a twisting cylinder. *Ain Shams Engineering Journal*, 14(2):101869, 2023. doi: 10.1016/j.asej.2022.101869.

[32] T. Bucha and K.P. Madasu. Slow flow past a weakly permeable spheroidal particle in a hypothetical cell. *Archive of Mechanical Engineering*, 68:119–146, 2021. doi: 10.24425/ame.2021.137044.

[33] K.P. Madasu and P. Sarkar. Couple stress fluid past a sphere embedded in a porous medium. *Archive of Mechanical Engineering*, pages 5–19, 2022. doi: 10.24425/ame.2021.139314.

[34] A. Kumar and K.P. Madasu. Non-newtonian fluid flow between parallel plates filled with an anisotropic porous medium. *Archive of Mechanical Engineering*, pages 273–294, 2024. doi: 10.24425/ame.2024.150565.

[35] M.S. Faltas and E.I. Saad. Thermophoresis-Brinkman flow of an aerosol particle within a spherical cavity. *Physics of Fluids*, 35(6):063121, 2023. doi: 10.1063/5.0156137.

[36] M.S. Faltas and K.E. Ragab. Thermophoresis of cylindrical particle immersed in Brinkman fluid. *Colloid Journal*, 83(6):676–687, 2021. doi: 10.1134/S1061933X2106003X.

[37] M. Ayman, E.I. Saad, and M.S. Faltas. Influence of concentration on thermophoresis of spherical aerosol particles within a brinkman medium. *Fluid Dynamics Research*, 56(5):055505, 2024. doi: 10.1088/1873-7005/ad8306.

[38] M.S. Faltas, H.H Sherief, and M.M. Ismail. Thermophoresis migration of an aerosol spherical particle embedded in a brinkman medium at small non-zero péclet numbers. *Physics of Fluids*, 35(8):083112, 2023. doi: 10.1063/5.0160402.

[39] S. El-Sapa. Effect of permeability of Brinkman flow on thermophoresis of a particle in a spherical cavity. *European Journal of Mechanics - B/Fluids*, 79:315–323, 2020. doi: 10.1016/j.euromechflu.2019.09.017.

[40] D.A. Nield, A. Bejan, et al. *Convection in porous media*. Springer, 2006.

[41] K.P. Madasu and T. Bucha. MHD viscous flow past a weakly permeable cylinder using happel and kuwabara cell models. *Iranian Journal of Science and Technology, Transactions A: Science*, 44(4):1063–1073, 2020. doi: 10.1007/s40995-020-00894-4.

[42] P.K. Yadav. Slow motion of a porous cylindrical shell in a concentric cylindrical cavity. *Meccanica*, 48:1607–1622, 2013. doi: 10.1007/s11012-012-9689-0.

[43] K.P. Madasu and D. Srinivasacharya. Micropolar fluid flow through a cylinder and a sphere embedded in a porous medium. *International Journal of Fluid Mechanics Research*, 44(3):229–240, 2017. doi: 10.1615/InterJFluidMechRes.2017015283.

[44] L. Talbot, R.K. Cheng, R.W. Schefer, and D.R. Willis. Thermophoresis of particles in a heated boundary layer. *Journal of Fluid Mechanics*, 101(4):737–758, 1980. doi: 10.1017/S0022112080001905.